Band gaps and the Kelvin-Helmholtz instability

Tom Chou
Department of Biomathematics and Department of Mathematics, UCLA, Los Angeles, California 90095-1766, USA
(Received 30 September 2006; published 31 January 2007)

We consider the linear stability of two inviscid fluids, in the presence of gravity, sheared past each other and separated by a flexible plate. Conditions for exponential growth of velocity perturbations are found as functions of the flexural rigidity of the plate and the shear rate. This Kelvin-Helmholtz instability is then analyzed in the presence of plates with spatially periodic (with period a) flexural rigidity arising from, for example, a periodic material variation. The eigenvalues of this periodic system are computed using Bloch's theorem (Floquet theory) that imposes specific Fourier decompositions of the velocity potential and plate deformations. We derive the non-Hermitian matrix whose eigenvalues determine the dispersion relation. Our dispersion relation shows that plate periodicity generally destabilizes the flow, compared to a uniform plate with the same mean flexural rigidity. However, enhanced destabilization and stabilization can occur for disturbances with wavelengths near an even multiple of the plate periodicity. The sensitivity of flows with such wavelengths arises from the nonpropagating, "Bragg reflected" modes coupled to the plate periodicity through the boundary condition at the plate.

DOI: 10.1103/PhysRevE.75.016315 PACS number(s): 47.20.Ft, 83.60.Wc, 46.70.De

I. INTRODUCTION

When two immiscible fluids are sheared relative to each other, the flow, and the normally flat interface between them, may become unstable. This classical Kelvin-Helmholtz instability arises from perturbations of the fluid velocity that grows into a vortex sheet due to local Bernoulli variations in pressure [1,2]. The presence of gravity also tunes this instability, depending on the mass density difference and shear rate between the two fluids. If the denser fluid is in lower gravitational potential, there is a critical shear rate beyond which small perturbations grow exponentially. This instability first arises in modes of the fluid velocity perturbation that have wave vectors greater than a critical wave vector. However, very small wavelength perturbations can be stabilized if additional restoring forces from, say, an interfacial surface tension [2], or a separating elastic plate are included. The Kelvin-Helmholtz instability has been thoroughly studied on all length scales; for example, in the context of knotting in astrophysical jets [3], cloud top entrainment instabilities [4], magnetohydrodynamic instabilities [1,5], the flutter of panels [6], and flow over a Langmuir monolayer [7]. Applications also arise in the general context of fluid solid interactions, particularly in bridges under wind loading [8,9].

Under the context of potential applications involving fluid-structure interactions, we consider the Kelvin-Helmholtz instability in the presence of an infinitesimally thin bendable plate separating the two inviscid flows, as shown in Fig. 1. We assume the plate is thin and inextensible, such that only bending modes can be excited. Since elastic restoring forces stabilize short wavelength perturbations, instabilities arise only for perturbations that have wave vectors within a certain window of values. Furthermore, we consider an elastic membrane that has spatially periodic properties, such as mass density or bending rigidity, which might arise, for example, in an engineered composite structure. By itself (in the absence of fluid), a periodic plate supports stable bending waves that propagate *except* at band gaps, i.e., frequencies corresponding to waves that have half-integer wavelengths in one period of the structural variation [10,11]. Waves near these wavelengths have vanishing group velocities and do not propagate in an infinite periodic medium due to their multiple "Bragg" reflections and deconstructive interference. Properties of wave propagation through periodic media have been computed in numerous physical settings, including acoustic waves moving through materials with periodic sound speeds [12], electromagnetic propagation through periodic dielectrics [11], and water wave propagation over periodic structures [13–19].

In this paper, we combine the periodic stabilizing membrane with an otherwise unstable shear flow and study the complex dispersion relation. A velocity perturbation with any wave vector, convected by the base laminar flow forms a traveling wave. This traveling wave, when coupled to the intrinsic periodicity of the elastic plate may be Bragg reflected and not able to propagate within the region of periodicity, altering its stability characteristics. In order to explore this heuristic argument further, we formulate in the next section the linear problem in terms of a vorticity-free velocity perturbation and a small deformation of the separating elastic membrane. We review, in turn, a uniform plate subject to destabilizing flow, and a free periodic plate that supports stable waves. The fully coupled problem, a periodic

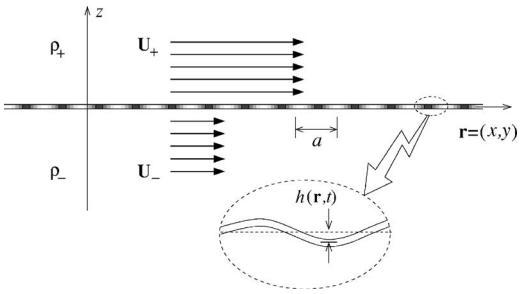

FIG. 1. Discontinuous shear flow separated by a periodically flexible plate.

plate in destabilizing flow, is then presented in the Results section. We show that the stability properties are affected most when the wavelengths of the most unstable modes are close to the periodicity of the plate flexibility. Implications and extensions to related flow systems are discussed in the Discussion and Conclusions section.

II. LINEAR MODEL

Consider the fluid-structure interaction depicted in Fig. 1. Two incompressible fluids flowing uniformly in two different directions, $\mathbf{U}_+$ and $\mathbf{U}_-$, in the x-y plane are separated by a negligibly thin elastic plate. Gravitational acceleration is in the $-\mathbf{z}$ direction and the fluid density above and below the plate are denoted $\rho_\pm$. Since viscosity will be neglected, we will consider only potential flows. The total velocity in each region $(\pm)$ is defined by the uniform flow $\mathbf{U}_\pm$ plus a small irrotational perturbation $\mathbf{v}_\pm \equiv \boldsymbol{\nabla}\varphi_\pm$. Upon imposing incompressibility, the upper and lower velocity potentials, $\varphi_\pm$, satisfy Laplace's equation,

$$(\nabla_\perp^2 + \partial_z^2)\varphi_\pm(\mathbf{r},z,t) = 0, \quad \nabla_\perp^2 = \partial_x^2 + \partial_y^2. \tag{1}$$

Since $\partial_z\varphi_\pm|_{z=0} \approx v_z$ is the vertical velocity of the surface, the linearized kinematic conditions at the plate-separated interface are

$$\partial_t h(\mathbf{r},t) + \mathbf{U}_\pm \cdot \boldsymbol{\nabla}_\perp h(\mathbf{r},t) - \lim_{\varepsilon\to 0} \partial_z\varphi_\pm(\mathbf{r}, \pm\varepsilon, t) = 0, \tag{2}$$

where $h(\mathbf{r},t)$ is the normal displacement of the plate. The linearized normal stress balance at the interface, including the normal forces arising from the flexible plate, is [20]

$$\begin{aligned}[\rho\dot{\varphi} + \rho\mathbf{U}\cdot\boldsymbol{\nabla}_\perp\varphi + \rho g h(\mathbf{r},t)]_-^+ &= m(\mathbf{r})\ddot{h}(\mathbf{r},t) + \nabla_\perp^2[D(\mathbf{r})\nabla_\perp^2]h(\mathbf{r},t) - [(1-\nu)D]_{xx}h_{yy} \\ &\quad - [(1-\nu)D]_{yy}h_{xx} + 2[(1-\nu)D]_{xy}h_{xy},\end{aligned} \tag{3}$$

where $[X]_-^+ \equiv \lim_{\varepsilon\to 0} X(z=\varepsilon) - X(z=-\varepsilon)$, and $\nu(\mathbf{r})$ is Poisson's ratio. In Eq. (3), $m(\mathbf{r})$ and $D(\mathbf{r})$ are the mass per unit area and the flexural rigidity of the plate, respectively [29,21]. We exclude irrelevant constant shifts in h and φ by considering only the nonzero wave-vector decompositions of the plate displacement and velocity potential,

$$h(\mathbf{r},t) = \sum_{\mathbf{q}\neq 0} \int_{-\infty}^{\infty} h_{\mathbf{q}}(\omega) e^{i\mathbf{q}\cdot\mathbf{r} - i\omega t} \frac{d\omega}{2\pi}$$

and

$$\varphi_\pm(\mathbf{r},z,t) = \sum_{\mathbf{q}\neq 0} \int_{-\infty}^{\infty} \varphi_{\mathbf{q}}^\pm(\omega) e^{i\mathbf{q}\cdot\mathbf{r} - i\omega t \mp |\mathbf{q}|z} \frac{d\omega}{2\pi}. \tag{4}$$

In Eqs. (4), we have also assumed a continuous time-harmonic decomposition. The representation of $\varphi_\pm(\mathbf{r},z,t)$ automatically satisfies Eq. (1) and the boundary conditions at $z \to \pm\infty$.

Henceforth, for simplicity, we assume that the Poisson's ratio is spatially uniform and take only the mass density and bending rigidity to be spatially periodic. Periodic plate mass density and rigidity functions obey $m(\mathbf{r}) = m(\mathbf{r}+\mathbf{R})$ and $D(\mathbf{r}) = D(\mathbf{r}+\mathbf{R})$, where $\mathbf{R} = n_1 a_1 \mathbf{e}_1 + n_2 a_2 \mathbf{e}_2$ (n_1, n_2 integers) is any basis vector describing the periodicity. Here, a_1, a_2 are the periodicities of $m(\mathbf{r})$ and $D(\mathbf{r})$ in the $\mathbf{e}_1, \mathbf{e}_2$ directions. The periodic functions $m(\mathbf{r})$ and $D(\mathbf{r})$ can thus be decomposed into a Fourier sum over reciprocal lattice vectors $\mathbf{G}$,

$$m(\mathbf{r}) = \sum_{\mathbf{G}} m(\mathbf{G}) e^{i\mathbf{G}\cdot\mathbf{r}} \quad \text{and} \quad D(\mathbf{r}) = \sum_{\mathbf{G}} D(\mathbf{G}) e^{i\mathbf{G}\cdot\mathbf{r}}. \tag{5}$$

The reciprocal lattice vectors $\mathbf{G} = n_1\mathbf{G}_1 + n_2\mathbf{G}_2$ are defined by the reciprocal lattice basis vectors

$$\mathbf{G}_1 = \frac{2\pi}{a_1}\frac{\mathbf{e}_2 \times \hat{\mathbf{z}}}{\mathbf{e}_1 \cdot (\mathbf{e}_2 \times \hat{\mathbf{z}})} \quad \text{and} \quad \mathbf{G}_2 = \frac{2\pi}{a_2}\frac{\hat{\mathbf{z}} \times \mathbf{e}_1}{\mathbf{e}_1 \cdot (\mathbf{e}_2 \times \hat{\mathbf{z}})}. \tag{6}$$

Finally, we assume a large plate with dimensions $L_1 \times L_2$ that fit an integer multiple of the period ($L_1 = N_1 a_1$ and $L_2 = N_2 a_2$) and impose periodic boundary conditions on the entire system: $m(\mathbf{r} + N_i a_i \mathbf{e}_i) = m(\mathbf{r})$ and $D(\mathbf{r} + N_i a_i \mathbf{e}_i) = D(\mathbf{r})$ for $i = 1, 2$. Under this construction, the wave-vector sum in the decompositions (4) are taken over $\mathbf{q} = \Sigma_{n_i \neq 0}(n_i/N_i)\mathbf{G}_i$. In the $L_1, L_2 \to \infty$ limit, sums over $\mathbf{q}$ become the Cauchy principal value of the corresponding Riemann integral.

After substitution of Eqs. (4) into the kinematic conditions (2), we find the relationship

$$\varphi_{\mathbf{q}}^\pm(\omega) = \pm \frac{i(\omega - \mathbf{U}_\pm \cdot \mathbf{q})}{|\mathbf{q}|} h_{\mathbf{q}}(\omega), \quad \mathbf{q} \neq 0. \tag{7}$$

Upon substitution of Eqs. (4), (5), and (7) into Eq. (3), and exploiting the orthogonality of the $e^{i\mathbf{q}\cdot\mathbf{r}}$ basis functions,

$$\begin{aligned}&[(\rho_+ + \rho_-)\omega^2 - 2\omega(\rho_+\mathbf{U}_+ + \rho_-\mathbf{U}_-)\cdot\mathbf{q} + \rho_+(\mathbf{q}\cdot\mathbf{U}_+)^2 \\ &\quad + \rho_-(\mathbf{q}\cdot\mathbf{U}_-)^2 + (\rho_+ - \rho_-)g|\mathbf{q}|]h_{\mathbf{q}} \\ &= -\omega^2|\mathbf{q}|\sum_{\mathbf{G}} m(\mathbf{G})h_{\mathbf{q}-\mathbf{G}} + \sum_{\mathbf{G}} |\mathbf{q}|^3|\mathbf{q}-\mathbf{G}|^2 D(\mathbf{G})h_{\mathbf{q}-\mathbf{G}} \\ &\quad - (1-\nu)|\mathbf{q}||\mathbf{G}\times(\mathbf{q}-\mathbf{G})|^2 h_{\mathbf{q}-\mathbf{G}}.\end{aligned} \tag{8}$$

Equation (8) shows that each coefficient $h_{\mathbf{q}}$ is linked with $N_1 \times N_2$ other coefficients $h_{\mathbf{q}-\mathbf{G}'}$. This problem can be solved numerically by truncating $h_{\mathbf{q}-\mathbf{G}} \approx 0$ for large $|\mathbf{G}|$ where $m(\mathbf{G})$ and $D(\mathbf{G})$ are small. Alternatively, Eq. (8) can be organized according to the "reduced zone scheme," by defining $\mathbf{k} = \mathbf{q} + \mathbf{G}$, where $\mathbf{G}$ is such that $\mathbf{k}$ is restricted in the first Brillouin zone defined by $|\mathbf{k}\cdot\mathbf{e}_i| < |\mathbf{G}_i\cdot\mathbf{e}_i|/2$ [10]. In this representation, we need only consider the $N_1 \times N_2$ eigenvalues, each with index $\mathbf{k}$ inside the first Brillouin zone. The problem is thus cast into a quadratic eigenvalue problem defined by

$$\sum_{\mathbf{G}'} [A_{\mathbf{k}}(\mathbf{G},\mathbf{G}')\omega^2 + B_{\mathbf{k}}(\mathbf{G},\mathbf{G}')\omega + C_{\mathbf{k}}(\mathbf{G},\mathbf{G}')]h_{\mathbf{k}-\mathbf{G}'}(\omega) = 0, \tag{9}$$

where

$$A_{\mathbf{k}}(\mathbf{G},\mathbf{G}') = \frac{\rho_+ + \rho_-}{|\mathbf{k}-\mathbf{G}|}\delta_{\mathbf{G},\mathbf{G}'} + m(\mathbf{G}'-\mathbf{G}),$$

$$B_{\mathbf{k}}(\mathbf{G},\mathbf{G}') = -2\left[\rho_+\frac{\mathbf{U}_+\cdot(\mathbf{k}-\mathbf{G})}{|\mathbf{k}-\mathbf{G}|} + \rho_-\frac{\mathbf{U}_-\cdot(\mathbf{k}-\mathbf{G})}{|\mathbf{k}-\mathbf{G}|}\right]\delta_{\mathbf{G},\mathbf{G}'},$$

$$C_{\mathbf{k}}(\mathbf{G},\mathbf{G}') = \left[\rho_+\frac{(\mathbf{U}_+\cdot(\mathbf{k}-\mathbf{G}))^2}{|\mathbf{k}-\mathbf{G}|} + \rho_-\frac{(\mathbf{U}_-\cdot(\mathbf{k}-\mathbf{G}))^2}{|\mathbf{k}-\mathbf{G}|} + (\rho_+ - \rho_-)g\right]\delta_{\mathbf{G},\mathbf{G}'} - [|\mathbf{k}-\mathbf{G}|^2|\mathbf{k}-\mathbf{G}'|^2 - (1-\nu)|\mathbf{G}\times(\mathbf{k}-\mathbf{G}')|^2]D(\mathbf{G},\mathbf{G}'). \quad (10)$$

Equation (9) is a matrix equation for $h_{\mathbf{k}-\mathbf{G}}(\omega)$ that has solutions for only certain $\omega(\mathbf{k})$. The full dispersion relation can be recovered by assigning the appropriate translation $\mathbf{G}$ in the eigenvalues $\omega(\mathbf{k}-\mathbf{G})$ to $\omega(\mathbf{q})$ for wave vectors $\mathbf{q}$ outside the first Brillouin zone. The system becomes unstable when $\omega(\mathbf{q})$ acquires an imaginary component.

In anticipation of a length scale a associated with the periodicity in the plate properties, we henceforth nondimensionalize all parameters and eliminate ρ_-, g, and a according to

$$\mathbf{r}\to\mathbf{r}/a, \quad \mathbf{G}\to a\mathbf{G}, \quad \mathbf{k}\to a\mathbf{k}, \quad \omega\to\sqrt{\frac{a}{g}}\omega,$$

$$\mathbf{U}_\pm\to\frac{\mathbf{U}_\pm}{\sqrt{ag}},$$

$$D\to\frac{D}{a^4\rho_- g}, \quad m\to\frac{m}{a\rho_-}, \quad \text{and } h_{\mathbf{k}}(\mathbf{G})\to h_{\mathbf{k}}(\mathbf{G})/a. \quad (11)$$

A. A uniform plate in the presence of flow

First consider the standard Kelvin-Helmholtz instability in the presence of a uniform elastic plate, where $m=m_0$ and $D(\mathbf{r})=D_0$ are constants. Miles [22] treated a similar problem of a thin boundary layer over an elastic plate. An elastic interface, with surface tension has also been studied in the context of flow over a lipid monolayer over an air-water interface [7]. For a uniform plate, $D(\mathbf{G})=D_0\delta_{\mathbf{G},0}$ and $m(\mathbf{G})=m_0\delta_{\mathbf{G},0}$, Eq. (9) is diagonal and is satisfied when

$$\Gamma(q)\omega_\pm(\mathbf{q}) = (\gamma\mathbf{U}_+ + \mathbf{U}_-)\cdot\mathbf{q} \pm \sqrt{\Delta(\mathbf{q})}, \quad (12)$$

where $\Gamma(q)\equiv\gamma+1+m_0q$, and the discriminant

$$\Delta(\mathbf{q}) \equiv \Gamma(q)[D_0q^5 + (1-\gamma)q] - \gamma((\mathbf{U}_+ - \mathbf{U}_-)\cdot\mathbf{q})^2 - m_0q(\gamma(\mathbf{U}_+\cdot\mathbf{q})^2 + (\mathbf{U}_-\cdot\mathbf{q})^2). \quad (13)$$

The eigenvalues $\omega_\pm$ become complex when $\Delta(\mathbf{q})$ becomes negative, leading to exponentially growing perturbations. In the limit where the influence of the plate is negligible $(m_0, D_0\approx 0)$ the dispersion relation reduces to that of the standard Kelvin-Helmholtz instability. The inclusion of membrane stiffness $(D_0>0)$ tends to stabilize small wavelength modes. For any given $m_0\geq 0$, the pairs of critical D_0 and U (denoted D_* and U_*) that give the onset of instability

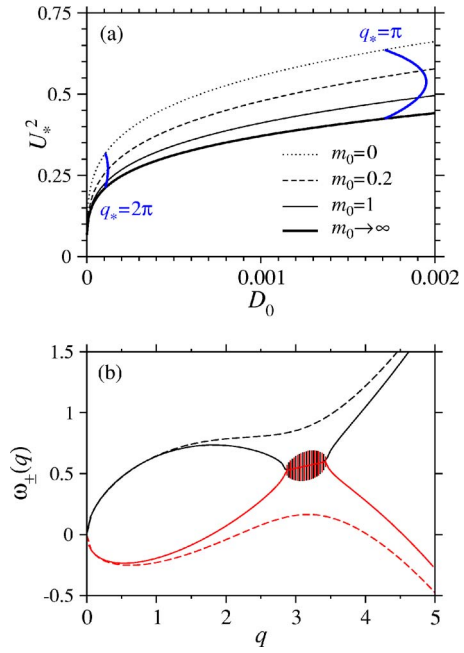

FIG. 2. (Color online) (a) The curve relating the critical value of the shear U_* to the constant flexural rigidity D_0, for various values of the uniform plate mass density m_0. For velocities greater than U_*, the flow becomes unstable. For different plate mass densities, the sets of D_*, U_* that give rise to an initial instability at wave vectors $q_*=\pi$ and $q_*=2\pi$ are shown by the black arcs spanning the curves. (b) The dispersion relation for a uniform plate just after the onset of instability.

at a chosen wave vector q_* can be expressed explicitly in two flow configurations where $\mathbf{U}_\pm$ and the $\mathbf{q}$ corresponding to the most unstable velocity perturbations are all collinear. When $\mathbf{U}_\pm$ are collinear, the onset of instability arises when $\Delta(\mathbf{q})=0$ is solved by two critical repeated, real roots, q_*, in addition to the root at $q=0$ and two complex conjugate roots. For a static configuration of the lower fluid ($\mathbf{U}_-=0$ in the reference frame of the plate), we find

$$D_* = \frac{(1+m_0q_*)^2 - \gamma^2(1+2m_0q_*) - \gamma m_0^2q_*^2}{q_*^4[3(1+\gamma+m_0^2q_*^2) + 2(\gamma+3)m_0q_*]},$$

$$U_*^2 = \frac{4(1-\gamma)(1+\gamma+m_0q_*)^2}{\gamma q_*[3(1+\gamma+m_0^2q_*^2) + 2(\gamma+3)m_0q_*]}. \quad (14)$$

Alternatively, for a chosen value of D_0, the critical U_* and the corresponding initially unstable wave vector can be found implicitly. The critical velocities U_*, as a function of D_0 and m_0 are shown in Fig. 2(a). Note that the critical velocity U_* *decreases* as the plate mass density m_0 increases. The limit $m_0\to\infty$ is different from the $\rho_\pm\to 0$ limit treated in the next section. Here, the plate flexibility remains constant as its mass density increases. Although the magnitude of $\omega_\pm(q)$ decreases, the discriminant [Eq. (13)] becomes negative at smaller U_* due to the increased inertial forces of the plate back on the fluid.

The two branches of the full dispersion relation $\omega_{\pm}(q)$ are plotted in Fig. 2(b). We have chosen parameters [$D_*(\pi)$ and U_*^2 defined by Eqs. (14)] such that the onset of instability arises at $q_* \approx \pi$. For $U=1/\sqrt{2} < U_*(q_*=\pi)=0.756\,320$, $\omega_{\pm}(q)$ are real, as shown by the dashed curves. We also plot (solid curves) the dispersion relation for $U=0.761\,577 > U_*(q_*=\pi)=0.756\,32$, whereupon a window of instability opens near $q_*=\pi$. The magnitude of the complex parts of $\omega_{\pm}(q)$ are indicated by the height of the shaded region.

In the second flow configuration, we assume a vanishing net momentum in the reference frame of the plate, $\mathbf{U}_-=-\gamma\mathbf{U}_+$. In this case, we find independent of m_0,

$$D_* = \frac{1-\gamma}{3q_*^4} \quad \text{and} \quad U_*^2 = \frac{4(1-\gamma)}{3\gamma(\gamma+1)q_*}, \tag{15}$$

and the symmetry $\omega_+(q)=-\omega_-(q)$. For $D_0 \lesssim D_*$ and/or $U \gtrsim U_*$, as defined by Eq. (14) or Eq. (15), $\omega(q \approx q_*)$ becomes complex and instability arises for a small window of wave vectors near q_*.

B. Dispersion relation for a free periodic plate

Now consider the limit of an isolated (but periodically structured) plate where the inertia of the bounding fluid is negligible. If the plate were uniform, the dispersion relation in the limit $\rho_{\pm} \to 0$ is simply $m_0\omega^2 = D_0 q^4$. For a periodically structured plate $[m(\mathbf{G}\neq 0)\neq 0, D(\mathbf{G}\neq 0)\neq 0]$, the dispersion relation can be found from Eq. (9). Henceforth, we assume the periodicities in the plate to be sinusoidal in the $\mathbf{x}$ direction and take the forms

$$m(\mathbf{r}) = m_0 + 2m_1 \cos 2\pi x, \quad D(\mathbf{r}) = D_0 + 2D_1 \cos 2\pi x. \tag{16}$$

The assumption of one-dimensional periodicity simplifies the analysis since all terms in Eqs. (3), (8), and (10) explicitly depending on ν vanish. Although the mean mass density and bending rigidity are unchanged from m_0 and D_0, respectively, the variations m_1 and/or D_1 will change the dispersion relation. Specifically, periodic variations will break the dispersion relation at wave vectors corresponding to waves that cannot propagate through an infinite, periodic medium. At each of these wave vectors (the "Bragg planes"), the waves (half-integers of which fit into a period) become standing. Corresponding to these nonpropagating waves are gaps in the frequency (band gaps, or stop bands) within which an infinitely periodic material cannot be excited.

Figures 3(a) and 3(b) show the dispersion relation of an isolated plate with periodicities in the bending rigidity (a), and mass density (b). The frequency gaps increase as the contrast m_1 or D_1 is increased. From consideration of the eigenvectors, the standing modes near the band gaps can be shown to have either nodes or antinodes over the high flexural rigidity (or high mass density) regions, depending on which side of the band gap the wave vector q lies. These behavior generally arise in wave propagation through periodic media. When the plate is coupled to flow, it will be the near equal-wavelength modes immediately straddling the band gaps, with different frequencies and ~90° out of phase, that will qualitatively affect the stability near the band gaps.

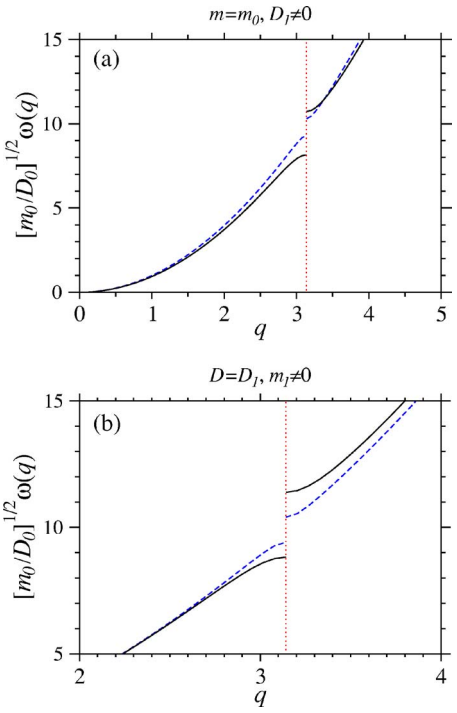

FIG. 3. (Color online) (a) The normalized dispersion relation $\sqrt{m_0/D_0}\omega_{\pm}(q)$ for $m_1=0$, $D_1/D_0=0.1$ (dashed curve) and $D_1/D_0=0.25$ (solid curve). (b) A blow-up of the dispersion relation for $D_1=0, m_1/m_0=0.1$ (dashed curve) and $m_1/m_0=0.25$ (solid curve).

III. RESULTS FOR THE COUPLED PROBLEM

We now combine the known results of the preceding sections and consider the fully coupled problem where fluid instabilities and Bragg reflection interact. For simplicity, we consider the plate periodicity wave vectors ($\mathbf{G}=2\pi n/a\hat{\mathbf{x}}$) and the uniform flows $\mathbf{U}_{\pm}=U_{\pm}\hat{\mathbf{x}}$ to be aligned. In the full problem, the dispersion relation $\omega(q)$ may be both complex (signalling regions of instability) and discontinuous at band gaps where $(\partial\omega/\partial q)=0$. The full dispersion relation is found from solving the quadratic eigenvalue problem given by Eq. (9). This problem can be expressed in linear eigenvalue form,

$$(\mathbf{M} - \omega\mathbf{I}) \cdot \boldsymbol{\eta} = \mathbf{0}, \tag{17}$$

with $\eta=(\mathbf{h}_{\mathbf{k}}, \omega\mathbf{h}_{\mathbf{k}})^{\mathbf{T}}$, and

$$\mathbf{M} = \begin{pmatrix} \mathbf{0} & \mathbf{I} \\ -\mathbf{A}^{-1}\mathbf{C} & -\mathbf{A}^{-1}\mathbf{B} \end{pmatrix}. \tag{18}$$

The dispersion relation $\omega(\mathbf{k})$ is found from the eigenvalues of the non-Hermitian matrix $\mathbf{M}$. For the parameters explored, we find numerical convergence of the lowest handful of eigenvalues with 40 or fewer modes $\mathbf{G}, \mathbf{G}'$. Therefore, we truncate the system at approximately 60 modes (where $\mathbf{M}$ is a 120×120 matrix). This is more than sufficient to obtain numerical accuracy for the lower eigenvalues at all relevant

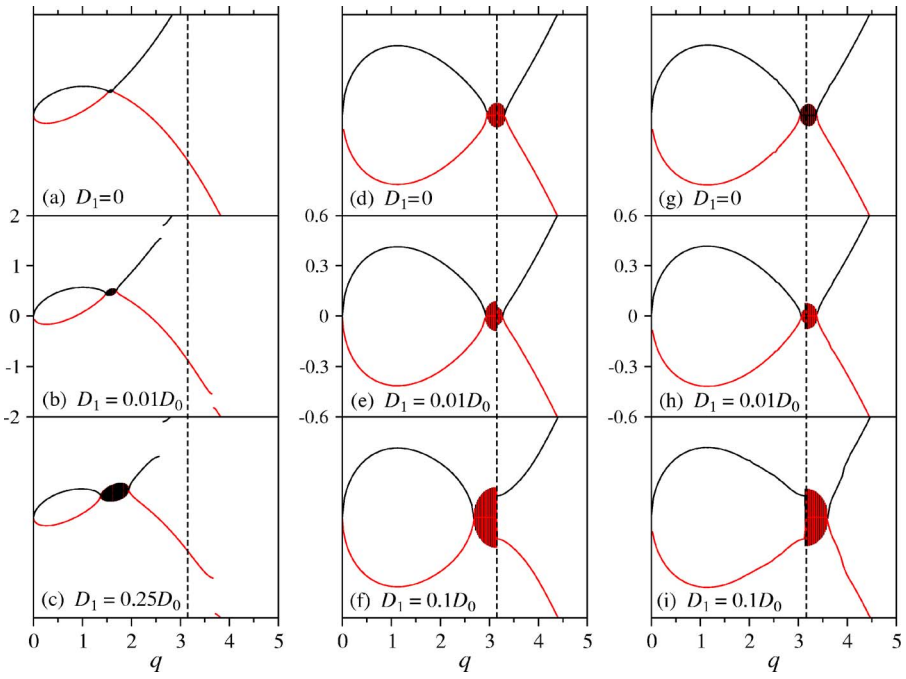

FIG. 4. (Color online) (a)–(c) The complex dispersion relation for a system just above the instability threshold. The instability is first triggered at $q_*=\pi/2$ (which arises for parameters $\gamma=1/2$, $m_0=0.2$, $D_0\leqslant D_*=0.029\,8349$, and $U^2\geqslant U_*^2=1.198\,09$). As D_1 increases, the instability bubble ($\mathrm{Im}\{\omega_\pm\}$) increases in size as more wave vectors become unstable. (d)–(f) Dispersion relation for instabilities that first arise at $q_*=3.14\lesssim\pi$. As D_1 is increased, the modes with $q<\pi$ are destabilized, while those with $q>\pi$ are stabilized. (g)–(i) Increasing D_1 when the incipient instability starts at $q_*=3.25>\pi$ destabilizes modes with $q>\pi$ and stabilizes those with $q<\pi$.

wave vectors. The eigenvalues of $\mathbf{M}$ are sorted from the numerical solutions and replotted in the extended zone scheme where the wave vector $0\leqslant|\mathbf{q}|<\infty$. When unfolding the eigenvalues $\omega(\mathbf{k})$, we make use of the fact the functions $\omega(0\leqslant|\mathbf{q}|<\infty)$ in the normal extended zone scheme come in pairs $\omega_\pm(\mathbf{q})$ and have the symmetry property $\omega_\pm(-|\mathbf{q}|)=-\omega_\mp(|\mathbf{q}|)$. This property, along with the consideration of the corresponding eigenvectors at each wave vector k allows us to reconstruct $\omega_\pm(q)$ from $\omega_\pm(k)$.

In Figs. 4(a)–4(c) we show the effects of increasing the strength of the periodic rigidity D_1/D_0 for the case $\mathbf{U}_-=0$. In Fig. 4(a) we show a system with an incipient instability at $q\approx q_*=\pi/2$.

As D_1 is increased [Figs. 4(b) and 4(c)] the bubble of instability grows modestly, while gaps in the dispersion relation also appear. The destabilizing effect of rigidities with periodicity $a\gg 2\pi/q_*$ can be understood in terms of a slight effective softening of the plate to bending modes with wavelengths greater than a [30].

Note that the gaps here do not appear at the Brillouin zone edge $q=\pi$ defined by a system's static periodic structure as in the free plate problem (Fig. 3) and in most other settings. Rather, they appear symmetrically around the band edge due to a doppler shift arising from the nonvanishing net momentum of the system. Gaps occurring away from the zone boundaries have been shown to arise in electromagnetic propagation through deformed cholesteric elastomers [23].

Now consider an incipient instability that arises at higher wave vectors, near the first band gap at $q=\pi$. Assume for simplicity, the zero net momentum ($\mathbf{U}_-=-\gamma\mathbf{U}_+$) case where $\mathbf{B}_\mathbf{k}(\mathbf{G},\mathbf{G}')=0$ in Eq. (9) and $\omega_\pm(q)=-\omega_\mp(q)$. Figures 4(d)–4(f) show the effects of increasing D_1 when the initial instability starts at $q_*=3.14\lesssim\pi$. As the plate heterogeneity is increased, modes with wave vector $q<\pi$ are destabilized, while those with $q>\pi$ are stabilized. Conversely, if the incipient instability arises at $q_*\gtrsim\pi$, as in Figs. 4(g)–4(i) (where $q_*=3.25$), increasing D_1 will destabilize modes with $q>\pi$, while stabilizing those with $q<\pi$. The discontinuous change in the eigenvalues across the Bragg plane $q=\pi$ occurs first in the imaginary component and the growth rate $\mathrm{Im}\{\omega(q)\}$ is discontinuous. As the contrast D_1/D_0 is further increased, $\mathrm{Re}\{\omega(q)\}$ also becomes discontinuous.

IV. DISCUSSION AND CONCLUSIONS

We have analyzed the properties of the instabilities of two fluids uniformly flowing past each other, separated by an elastic plate with periodic bending rigidity and/or mass density. Our generalization of the Kelvin-Helmholtz instability can be quantified by finding the eigenvalues and eigenvectors of a non-Hermitian matrix [Eq. (9)]. The imaginary components of the eigenvalues $\omega(q)$ determine the rate of unstable growth for eigenmodes of wave vector q. We find that an imposed plate periodicity generally destabilizes the flow but that the destabilization mainly occurs in the band of wave vectors on the side of the initially most unstable mode. Modes with wave vectors on the other side of the band gap from the most unstable wave vector q_* are stabilized as D_1 is increased.

The destabilization and/or stabilization that occurs on either side of the band gap can be understood in terms of $\sim 90°$ out-of-phase standing modes with wave vectors $q=(2n-1)\pi\pm\varepsilon$ immediately straddling the nth band gap. For example, if $q_*\gtrsim(2n-1)\pi$, increasing D_1 destabilizes the waves with $q\approx q_*$ since their antinodes occur predominantly over regions of lower rigidity. Modes with $q<(2n-1)\pi$, on the other side of the nth band gap, can be significantly stabilized since they are approximately 90° out-of-phase, and their antinodes sample a stiffer plate. The same argument applies for $q_*\lesssim(2n-1)\pi$.

Our results suggest possible stability control strategies. By adding restoring forces (such as bending rigidity) with

periodicity near the wavelength of the most unstable mode, stability can be enhanced or diminished at wavelengths either less than or greater than the band gap wavelength. Stabilization of specific modes against Kelvin-Helmholtz instabilities can be achieved, but at the expense of destabilization of other nearby modes.

In a recent experiment, the stability of an elastic flag in the presence of flow was mapped [24]. Although in the limit of uniform flags immersed in a single density fluid, the linear stability condition is identical to that defined by Eqs. (12) and (13), copper inserts were periodically inserted into the flag for support [24]. The flapping was of low enough wave vector that the copper inserts would only contribute to an effective mass and effective bending rigidity. However, for similar applications where the system is driven to be initially unstable for wavelengths comparable to the wavelength of the periodic material inhomogeneity, Eqs. (17) and (18) would apply.

Extensions of our approach to stability analysis in other fluid-structure systems should be possible. For example, the Orr-Sommerfeld problem [25] in nonuniform Poiseuille flow through periodically elastic pipes can be similarly solved. A physical realization of flow through elastically periodic pipes may have arisen in the experiments of Ref. [26] in which damping elements were periodically embedded along an elastic pipe. The Kelvin-Helmholtz-type instability has been only briefly mentioned in this context by Refs. [27,28], and only in uniform pipes. Moreover, the effects of periodicity on other classes of instabilities (e.g., Tollmien-Schlichting) have not been explored. It would also be interesting to consider the effects of dissipation, in both the fluid flow and the viscoelastic plate, on the stability properties of a periodic system.

ACKNOWLEDGMENTS

This work was supported by the US National Science Foundation through Grant No. DMS-0349195, and the US National Institutes of Health via Grant No. K25AI058672.

[1] S. Chandrasekar, *Hydrodynamic and Hydromagnetic Stability* (Clarendon, Oxford, 1961).
[2] G. B. Whitham, *Linear and Nonlinear Waves* (Wiley Interscience, New York, 1999).
[3] R. D. Blandford and M. J. Rees, Mon. Not. R. Astron. Soc. **169**, 395 (1974).
[4] N. M. Reiss and T. J. Corona, Bull. Am. Meteorol. Soc. **58**, 159 (1977).
[5] A. Frank, T. W. Jones, D. Ryu, and J. B. Gaalaas, Astrophys. J. **460**, 777 (1996).
[6] J. W. Miles, J. Aeronaut. Sci. **23**, 77 (1956).
[7] S. Komura and T. Iwayama, J. Phys. II **7**, 1331 (1997).
[8] D. G. Crighton and J. E. Oswell, Philos. Trans. R. Soc. London, Ser. A **335**, 557 (1991).
[9] X. Zhang and B. Sun, J. Wind. Eng. Ind. Aerodyn. **92**, 431 (2004).
[10] N. W. Ashcroft and N. D. Mermin, *Solid State Physics* (Thomson Learning, Inc., New York, 1976).
[11] J. Joannopolous, R. D. Meade, and J. N. Winn, *Photonic Crystals: Molding the Flow of Light* (Princeton University Press, Princeton, NJ, 1995).
[12] M. M. Sigalas and E. N. Economou, J. Sound Vib. **158**, 377 (1992).
[13] L. S. Chen, C. H. Kuo, Z. Ye, and X. Sun, Phys. Rev. E **69**, 066308 (2004).
[14] T. Chou, J. Fluid Mech. **369**, 333 (1998).
[15] X. Hu and C. T. Chan, Phys. Rev. Lett. **95**, 154501 (2005).
[16] X. Hu, Y. Shen, X. Liu, R. Fu, and J. Zi, Phys. Rev. E **68**, 066308 (2003).
[17] M. Naciri and C. C. Mei, J. Fluid Mech. **192**, 51 (1998).
[18] M. A. Peter, M. H. Meylan, and C. M. Linton, J. Fluid Mech. **548**, 237 (2006).
[19] R. Porter and D. V. Evans, Wave Motion **23**, 95 (1996).
[20] D. Porter and R. Porter, J. Fluid Mech. **509**, 145 (2004).
[21] L. D. Landau and E. M. Lifshitz, *Theory of Elasticity*, 3rd ed. (Maxwell Macmillan International, New York, 1989).
[22] J. Miles, J. Fluid Mech. **434**, 371 (2001).
[23] P. A. Bermel and M. Warner, Phys. Rev. E **65**, 056614 (2002).
[24] M. Shelley, N. Vandenberghe, and J. Zhang, Phys. Rev. Lett. **94**, 094302 (2005).
[25] S. A. Orszag, J. Fluid Mech. **50**, 689 (1971).
[26] M. O. Kramer, J. Am. Soc. Nav. Eng. **72**, 25 (1960).
[27] T. B. Benjamin, J. Fluid Mech. **9**, 513 (1960).
[28] M. T. Landahl, J. Fluid Mech. **13**, 609 (1961).
[29] For plates composed of a material homogeneous across its thickness, $m(\mathbf{r})=\rho_0(\mathbf{r})d(\mathbf{r})$ and $D(\mathbf{r})=E(\mathbf{r})d^3(\mathbf{r})/\{12[1-\nu(\mathbf{r})]\}$, where $\rho_0(\mathbf{r})$ is the local mass density of the plate material, $d(\mathbf{r})$ is the local plate thickness, and $E(\mathbf{r})$ is the local Young's modulus of the plate material [21].
[30] The effective long wavelength bending rigidity of a plate made from alternating equal strips of two materials with individual rigidities $D_0 \pm \Delta D$ is $D_{\text{eff}}=2/[1/(D_0+\Delta D)+1/(D_0-\Delta D)] \approx D_0-(\Delta D)^2/D_0$.